DOI: 10.1002/ange.201406219

Dinuclear Metal Complexes

Facile C–H Bond Formation by Reductive Elimination at a Dinuclear Metal Site**

Richard D. Adams, Vitaly Rassolov,* and Yuen Onn Wong*

Abstract: *The electronically unsaturated dirhenium complex* $[Re_2(CO)_8(\mu\text{-}AuPPh_3)(\mu\text{-}Ph)]$ (**1**) *was obtained from the reaction of* $[Re_2(CO)_8\{\mu\text{-}\eta^2\text{-}C(H){=}C(H)nBu\}(\mu\text{-}H)]$ *with* $[Au(PPh_3)Ph]$. *The bridging* $\{AuPPh_3\}$ *group was replaced by a bridging hydrido ligand to yield the unsaturated dirhenium complex* $[Re_2(CO)_8(\mu\text{-}H)(\mu\text{-}Ph)]$ (**2**) *by reaction of* **1** *with* $HSnPh_3$. *Compound* **2** *reductively eliminates benzene upon addition of NCMe at 25°C. The electronic structure of* **2** *and the mechanism of the reductive elimination of the benzene molecule in its reaction with NCMe were investigated by DFT computational analyses.*

The making and breaking of C–H bonds is fundamental to the transformations of organic molecules into new compounds.[1] In many cases, these transformations are facilitated by metal atoms via oxidative addition and reductive elimination processes.[2,3] The mechanisms of these processes at single metal atoms have been the subject of intense scrutiny over the years.[3,4] The nature of these processes on metal surfaces and at polynuclear metal centers is certainly more complex and is not as well understood, but it is certainly of no less importance.[5–7] Multicenter metal-based transformations of hydrocarbons are believed to be important in heterogeneous catalytic hydrogenations,[8] petroleum reforming,[9] and Fischer–Tropsch chemistry.[10]

There are strong similarities between the reductive elimination of C–H bonds and the reductive elimination of the H–H bond to form H_2. In 1984, Trinquier and Hoffmann showed that the concerted symmetric C_{2v} intramolecular, 1,2-reductive elimination of H_2 from a dinuclear metal center is a symmetry-forbidden process, but an unsymmetrical elimination via the planar C_s geometric form is symmetry-allowed (Scheme 1 A and B, respectively).[11]

In this work we have synthesized the complexes $[Re_2(CO)_8(\mu\text{-}AuPPh_3)(\mu\text{-}Ph)]$ (**1**) and $[Re_2(CO)_8(\mu\text{-}H)(\mu\text{-}Ph)]$ (**2**) containing a bridging phenyl ligand and a bridging gold-phosphine group (**1**) and a bridging hydrido ligand (**2**). When allowed to react with NCMe at room temperature, compound **2** readily eliminates benzene by a C–H bond forming reductive elimination of the bridging phenyl ligand and the bridging hydrido ligand. The mechanism of this elimination has been investigated and ascertained by DFT computational analyses and is reported herein.

The complex $[Re_2(CO)_8(\mu\text{-}AuPPh_3)(\mu\text{-}Ph)]$ (**1**) was obtained in 87% yield from the reaction of $[Re_2(CO)_8[\mu\text{-}\eta^2\text{-}C(H){=}C(H)nBu](\mu\text{-}H)]$ with $[Au(PPh_3)(Ph)]$. Compound **1** was characterized by a single-crystal X-ray diffraction analysis (see Supporting Information). An ORTEP diagram of the molecular structure of **1** is shown in Figure 1. The molecule contains two $\{Re(CO)_4\}$ groups held together by a bridging $\{AuPPh_3\}$ group, an η^1-bridging phenyl ligand and a strong Re–Re bonding interaction. The Re–Au distances

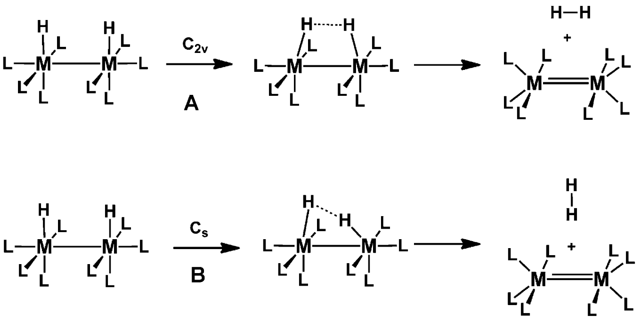

Scheme 1. Intramolecular dinuclear 1,2-reductive elimination.

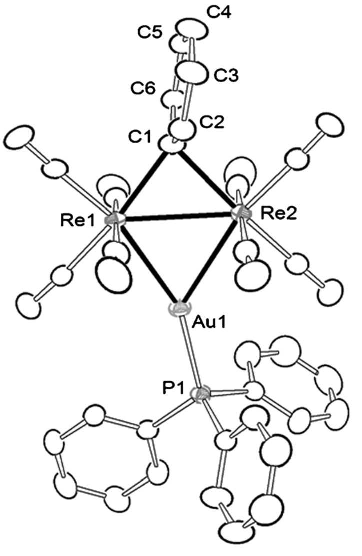

Figure 1. An ORTEP diagram of the molecular structure of $[Re_2(CO)_8(\mu\text{-}AuPPh_3)(\mu\text{-}Ph)]$ (**1**) showing 30% thermal ellipsoid probability. Selected interatomic bond distances [Å] are as follow: Re1–Re2 2.9690(4), Au1–Re1 2.7567(3), Au1–Re2 2.8080(4), Re1–C1 2.292(5), Re2–C1 2.396(5).

---

[*] Dr. R. D. Adams, Dr. V. Rassolov, Y. O. Wong
Department of Chemistry and Biochemistry
University of South Carolina
JM Palms Ctr for GSR, Columbia, SC 29208 (USA)
E-mail: ADAMSRD@mailbox.sc.edu

[**] Support for this research from the National Science Foundation (CHE-1111496 and CHE-1048629) is gratefully acknowledged.

Supporting information for this article is available on the WWW under http://dx.doi.org/10.1002/anie.201406219.

(Au1–Re1 2.7567(3) Å, Au1–Re2 2.8080(4) Å) and the Re–C distances to the bonded carbon atom of the bridging phenyl ligand (Re1–C1 2.292(5) Å, Re2–C1 2.396(5) Å) are slightly, but significantly different in the solid state. Compound **1** contains only 32 valence electrons at the two metal atoms and is thus formally electronically unsaturated by the amount of two electrons. Accordingly, the Re–Re distance is short (Re1–Re2 2.9690(4) Å) and is similar to that found in a related unsaturated complex, $[Re_2(CO)_8(\mu\text{-}AuPPh_3)_2]$ (Re1–Re2 2.9070(3) Å).[12]

When treated with $HSnPh_3$, compound **1** was converted into the new compound $[Re_2(CO)_8(\mu\text{-}H)(\mu\text{-}Ph)]$ (**2**) in 44% yield by replacement of the bridging $\{Au(PPh_3)\}$ group with a bridging hydrido ligand. Compound **2** was also characterized crystallographically (see Supporting Information) and an ORTEP diagram of its molecular structure is shown in Figure 2. Like **1**, compound **2** also has only 32 valence electrons and is also electronically unsaturated by the amount of two electrons. The Re–Re bond is only slightly longer than that in **1** (Re1–Re2 2.9924(3) Å) and the phenyl and hydrido ligands bridge the Re–Re bond asymmetrically in the solid state (Re1–H1 2.23(10) Å, Re2–H1 2.08(10) Å, Re1–C1 2.397(5) Å, Re2–C1 2.266(5) Å). This lack of symmetry may be a result of molecular packing in the solid state as the gas-phase DFT geometry-optimized structure is symmetrical (see below).

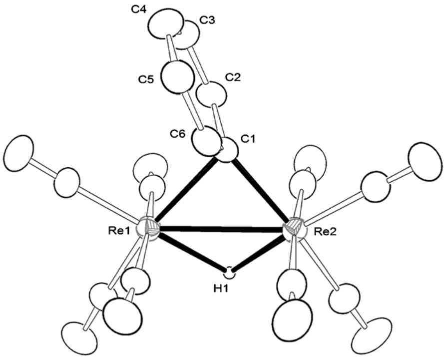

Figure 2. An ORTEP diagram of the molecular structure of $[Re_2(CO)_8(\mu\text{-}H)(\mu\text{-}Ph)]$ (**2**) showing 30% thermal ellipsoid probability. Selected interatomic bond distances [Å] and angles [°] are as follows: Re1–Re2 2.9924(3), Re1–H1 2.23(10), Re2–H1 2.08(10), Re1–C1 2.397(5), Re2–C1 2.266(5); Re2-H1-Re1 87.9(2), Re2-C1-Re1 79.80(17).

In order to understand the bonding in **2**, a gas-phase PBEsol geometry-optimized DFT calculation from the ADF computational package[13] of the structure of **2** was performed (see Supporting Information). This analysis provided a structure with equivalent Re–H distances (1.87 Å) and equivalent Re–C distances (2.32 Å) to the carbon atom of the bridging phenyl ligand, and the plane of the C_6 ring of the bridging phenyl ligand was perpendicular to that Re–Re vector. Molecular orbitals generated from these calculations show delocalized bonding across the *ipso*-carbon atom of the phenyl ring, the two rhenium atoms and the bridging hydride ligand (Figure 3). The computed HOMO–LUMO gap is 2.62 eV, a value smaller than the typical computed gaps in stable molecules, and is consistent with an unsaturated electronic structure.

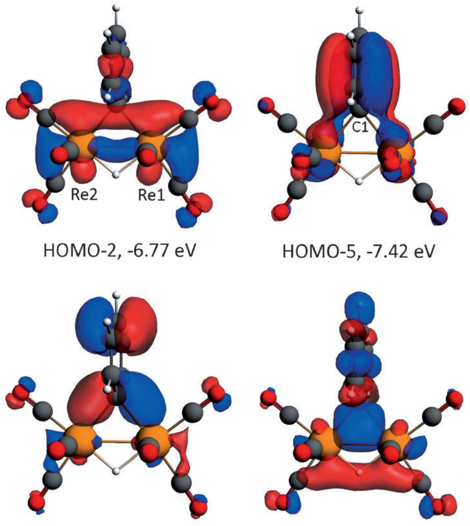

HOMO-2, -6.77 eV HOMO-5, -7.42 eV

HOMO-7, -7.75 eV HOMO-8, -8.07 eV

Figure 3. Selected molecular orbitals (MOs) with calculated energies in eV for compound **2** that show the nature of the bonding of the phenyl and hydrido ligands to the two rhenium atoms. The rhenium atoms are colored orange.

The HOMO−2 (−6.77 eV) shows a closed 3-center σ-type bond involving the phenyl carbon atom C1 and the two rhenium atoms. The HOMO−8 is predominantly a 4-center central interaction that includes the hydrido ligand, C1, and the two rhenium atoms. The HOMO−5 and HOMO−7 show the existence of electron donations from the filled π-orbitals of the phenyl ligand to the rhenium atoms which helps to reduce some of the electronic unsaturation at the Re atoms resulting in the longer Re–Re distances versus that in $[Re_2(CO)_8(\mu\text{-}AuPPh_3)_2]$. Note: the Re–Re distance in the unsaturated dirhenium compound $[Re_2(CO)_8(\mu\text{-}H)_2]$ at 2.876(1) Å is also significantly shorter than that in **1** and **2**.[14]

When treated with $[D_3]NCMe$ in an NMR tube, compound **2** was converted into $[Re_2(CO)_8([D_3]NCMe)_2]$ and benzene (C_6H_6) in essentially quantitative yield after 19 h at 25 °C.

A series of DFT computational analyses were performed in order to establish a mechanism for the formation of benzene from the bridging H and Ph ligands. This analysis shows that the transformation is induced by the approach of an NCMe ligand to one of the metal atoms and proceeds via a transition state **TS1** (+15.6 kcal mol^{-1}) as the nitrogen atom approaches the rhenium atom Re1 at 2.73 Å (see top of Figure 4).

At the same time, the Re1–C1 bond lengthens to 2.48 Å and the phenyl ligand begins to shift towards Re2 (Re2–C1 2.28 Å). The Re–Re bond also weakens to 3.02 Å, as the addition of electron density from the NCMe ligand reduces some of the electronic unsaturation at the metal atoms. The transformation proceeds to an intermediate, **I1**, −8.86 kcal mol^{-1} from **2**, as the Re–N bond (2.09 Å) to the NCMe ligand becomes fully established on Re1. At this time, the phenyl

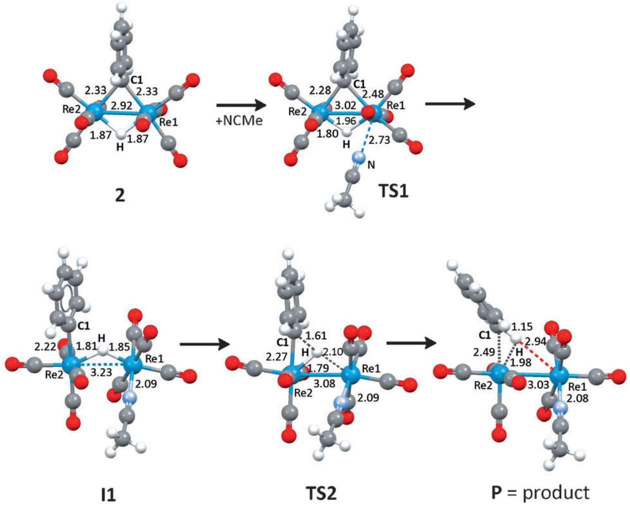

Figure 4. Structures of intermediates and transition states with selected interatomic distances that are traversed in the course of the NCMe-induced reductive elimination of benzene from **2**.

ligand has been shifted completely to a terminal coordination site on Re2 (Re2–C1 2.22 Å) (see Figure 4 bottom).

The hydride ligand remains as a bridge across the two Re atoms, but it has shifted to the other side of the Re–Re bond and lies *cis* to the phenyl ligand. The Re–Re bond has lengthened to 3.23 Å. The formation of the C–H bond proceeds by a shift of the bridging hydride ligand from the metal–metal bond to the carbon atom C1. This shift passes over a low-energy transition state, **TS2** (−4.30 kcal mol^{-1}) and would be virtually spontaneous in a solution at room temperature, that is, the addition of the second NCMe ligand to the complex is not needed to drive the formation of the C–H bond at this stage of the process. In **TS2**, the C1–H distance is 1.61 Å and the Re–Re bond has shortened to 3.08 Å as the hydride moves toward C1. The product, $[Re_2(CO)_8(NCMe)(\eta^2\text{-}C_6H_6)]$ (**P**), contains a η^2-CH bound benzene ligand terminally coordinated to Re2 (C1–H 1.15 Å, Re2–C1 2.49 Å, Re2–H 1.98 Å, and Re1–Re2 3.03 Å). The Re1⋯H distance, 2.94 Å, is a nonbonding interaction in this species (see Figure 4 bottom). An energy profile of the transformations along the reaction coordinate is shown in Figure 5.

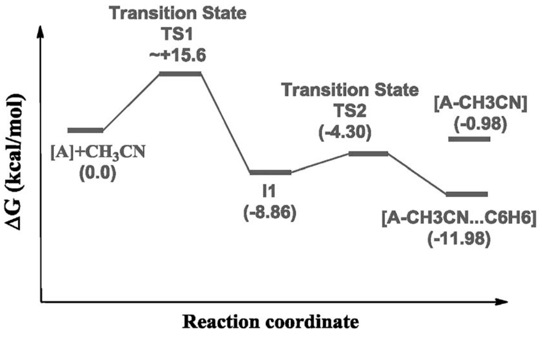

Figure 5. An energy profile of the transformations **2** along the reaction coordinate during the addition of NCMe. The energies in eV are given in parentheses.

Views of the molecular orbitals that show transformations in the bonding in the course of the C–H bond forming process are shown in Figure 6. The symmetric nature of the Re–C bonding to the phenyl ring at the beginning is nicely represented by the HOMO−2 shown in Figure 3. As the NCMe ligand begins to donate electron density to Re1, the Re–C bonding weakens as **TS1** is traversed (see the **TS1** HOMO−4, Figure 6). The HOMO−12 in **I1** shows the formation of an C1-H-Re1 overlap which is the predecessor to the C–H bond shown by the HOMO−15 in **TS2**. Finally, the C–H bond is fully formed as shown in the HOMO−10 in the η^2-benzene product complex **P**. Facile displacement of the benzene ligand by a second equivalent NCMe (not shown in

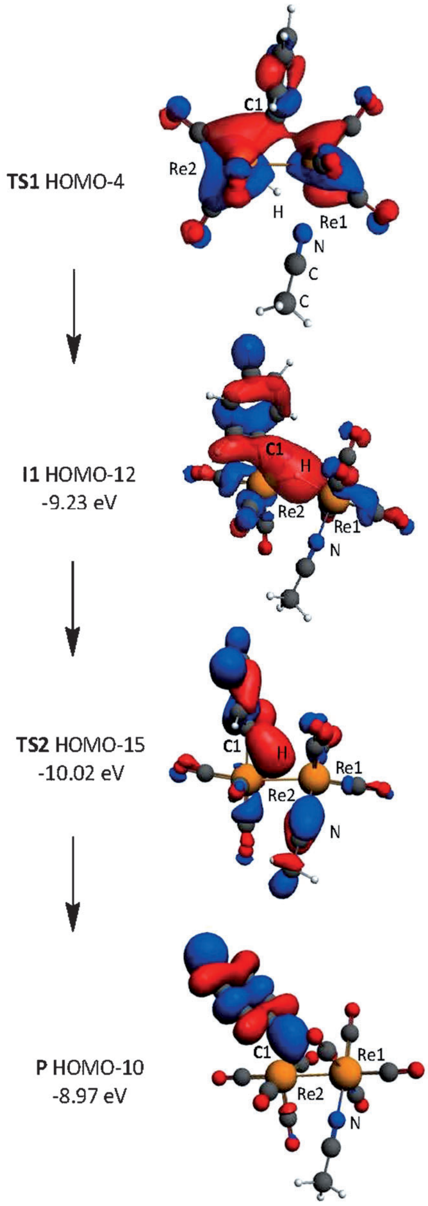

Figure 6. Selected molecular orbitals for **2** that emphasize the nature of the Re–C, Re–H and C–H bonding interactions in the course of the formation of the C–H bond during the reductive elimination process.

Figure 6) would complete the transformation as it occurs in solution.

Although the C–H bond forming process takes place predominantly at one metal atom only, Re2, the second Re atom is not completely a spectator, as the H atom is delivered to the carbon atom C1 from the Re–Re bond. It can be seen that the C–H bond forming process upon the addition of NCMe to **2**, at least in the final stages, strongly resembles that of the unsymmetric, planar reductive elimination of H_2 (path B in Scheme 1) that was predicted by Trinquier and Hoffmann 30 years ago.[11]

Despite the fact that it has not yet been observed in this system, it should not go unnoticed that the microscopic reverse of the **2** to **P** reaction is tantamount to a C–H bond activation process[2] and in this process the cleavage of the C–H bond would be facilitated by the second metal atom when the hydrogen atom is "inserted" into the Re–Re bond via the **TS2–I1** rearrangement. Furthermore, these results also may have important implications of C–H bond cleavage processes at multinuclear metal sites on metal nanoparticles[6] and metal surfaces[7] as the complete sequence takes place with only small changes in the metal–metal bond distances.

Experimental Section

40.0 mg (0.0745 mmol) of [Au(PPh$_3$)Ph] was added to 38.0 mg (0.0558 mmol) of [Re$_2$(CO)$_8$[μ-η^2-C(H)=C(H)*n*Bu](μ-H)] dissolved in 25 mL of hexane. The solution was refluxed for 3 h, dried in vacuo and the residue was separated by thin layer chromatography to provide pure yellow **1** in 87 % yield. 20.4 mg (0.0581 mmol) of HSnPh$_3$ was added to 44.0 mg (0.0388 mmol) of **1** dissolved in 25 mL of methylene chloride and stirred at room temperature for 1 h. The solution was dried in vacuo and the residue was separated by thin layer chromatography to provide pure yellow **2** in 44 % yield. Sn_2Ph_6 was a major coproduct.

Elimination of benzene from **2** was produced in essentially 100 % yield by dissolving **2** in [D$_3$]NCMe in an NMR tube and following the reaction by ^{1}H NMR spectroscopy for a period of 19 h.

Single-crystal structure determinations: The intensity data were collected by using a Bruker SMART APEX CCD-based diffractometer with Mo Kα radiation ($\lambda = 0.71073$ Å) at 294 K. All non-hydrogen atoms were refined with anisotropic thermal parameters. Hydrogen atoms were placed in geometrically idealized positions and included as standard riding atoms during the least-squares refinements.

Crystal data for **1**: $AuRe_2PO_8C_{32}H_{20}$, Monoclinic, $P2_1/c$, $M_r = 1132.82$ g mol^{-1}, $a = 14.401(2)$, $b = 24.572(3)$, $c = 9.1438(13)$ Å, $\alpha = 90.00$, $\beta = 95.440(3)$, $\gamma = 90.00°$, $V = 3221.0(8)$ Å^3, $Z = 4$, $\rho_{calcd} = 2.336$ g cm^{-3}, $\mu = 12.139$ mm^{-1}; $2\theta_{max} = 56.48°$, $F(000) = 2080$, $R_{int} = 0.0356$, no.collected/unique/$I_0 > 2\sigma I_0$ data = 39539/6950/5419, $R1/wR2$(all data) = 0.0224/0.0552, $R1/wR2(I_0 > 2\sigma I_0) = 0.0208/0.0542$), max./min. electron density = 0.526/−1.820 e$^-$ Å^{-3}.

Crystal data for **2**: $Re_2O_8C_{14}H_6$, Orthorhombic, $P2_12_12_1$, $M_r = 674.59$ g mol^{-1}, $a = 8.8587(4)$, $b = 12.7536(5)$, $c = 14.7467(6)$ Å, $\alpha = \beta = \gamma = 90.00°$, $V = 1666.09(12)$ Å^3, $Z = 4$, $\rho_{calcd} = 2.689$ g cm^{-3}, $\mu = 14.555$ mm^{-1}, $2\theta_{max} = 56.56°$, $F(000) = 1216$, $R_{int} = 0.0522$, no.collected/unique/$I_0 > 2\sigma I_0$ data = 20608/7220/2910, R1/*w*R2(all data) = 0.0187/0.0454, $R1/wR2(I_0 > 2\sigma I_0) = 0.0183/0.0450$), max./min. electron density = 0.357/−0.970 e$^-$ Å^{-3}.

CCDC 1014760 (**1**) and 1014761 (**2**) contain the supplementary crystallographic data for this paper. These data can be obtained free of charge from The Cambridge Crystallographic Data Centre via www.ccdc.cam.ac.uk/data_request/cif.

Received: June 13, 2014
Revised: July 13, 2014
Published online: August 21, 2014

Keywords: C–H bond formation · dinuclear metal site · reductive elimination · rhenium · unsaturated complexes

[1] G. A. Olah, A. Molnar in *Hydrocarbon Chemistry*, Wiley, New York, **1995**, pp. 1 – 25.

[2] a) R. H. Crabtree, *J. Organomet. Chem.* **2004**, *689*, 4083 – 4091; b) B. A. Vastine, M. B. Hall, *Coord. Chem. Rev.* **2009**, *253*, 1202 – 1218; c) C. Hall, R. N. Perutz, *Chem. Rev.* **1996**, *96*, 3125 – 3146; d) J. A. Labinger, J. E. Bercaw, *Nature* **2002**, *417*, 507 – 514.

[3] G. J. Kubas in *Metal Dihydrogen and Sigma Bond Complexes*, Kluwer, New York, **2002**, pp. 365 – 411.

[4] a) W. D. Jones, *Acc. Chem. Res.* **2003**, *36*, 140 – 246; b) G. Parkin, J. E. Bercaw, *Organometallics* **1989**, *8*, 1172 – 1179; c) G. L. Gould, D. M. Heinekey, *J. Am. Chem. Soc.* **1989**, *111*, 5502 – 5504.

[5] V. Ritleng, M. Checuti, *Chem. Rev.* **2007**, *107*, 797 – 858.

[6] a) F. Viñes, Y. Lykhach, T. Staudt, M. P. A. Lorenz, C. Papp, H.-P. Steinrück, J. Libuda, K. M. Neyman, A. Görling, *Chem. Eur. J.* **2010**, *16*, 6530 – 6539; b) Y.-H. Chin, C. Buda, M. Neurock, E. Iglesia, *J. Am. Chem. Soc.* **2013**, *135*, 15425 – 15442.

[7] J.-Y. Saillard, R. Hoffmann, *J. Am. Chem. Soc.* **1984**, *106*, 2006 – 2026.

[8] G. A. Olah, A. Molnar in *Hydrocarbon Chemistry*, Wiley, New York, **1995**, chap. 11, pp. 619 – 678.

[9] G. A. Olah, A. Molnar in *Hydrocarbon Chemistry*, Wiley, New York, **1995**, chap. 2, pp. 30 – 70.

[10] R. C. Brady, R. Pettit, *J. Am. Chem. Soc.* **1980**, *102*, 6181 – 6182.

[11] G. Trinquier, R. Hoffmann, *Organometallics* **1984**, *3*, 370 – 380.

[12] R. D. Adams, Y. O. Wong, Q. Zhang, *Organometallics* **2013**, *32*, 7540 – 7543.

[13] a) G. te Velde, F. M. Bickelhaupt, S. J. A. van Gisbergen, C. Fonseca Guerra, E. J. Baerends, J. G. Snijders, T. Ziegler, *J. Comput. Chem.* **2001**, *22*, 931 – 967; b) C. Fonseca Guerra, J. G. Snijders, G. te Velde, E. J. Baerends, *Theor. Chem. Acc.* **1998**, *99*, 391 – 403; c) J. P. Perdew, A. Ruzsinszky, G. I. Csonka, O. A. Vydrov, G. E. Scuseria, L. A. Constantin, X. Zhou, K. Burke, *Phys. Rev. Lett.* **2008**, *100*, 136406; d) J. P. Perdew, A. Ruzsinszky, G. I. Csonka, O. A. Vydrov, G. E. Scuseria, L. A. Constantin, X. Zhou, K. Burke, *Phys. Rev. Lett.* **2009**, *102*, 039902.

[14] a) M. J. Bennett, W. A. G. Graham, J. K. Hoyano, W. L. Hutcheon, *J. Am. Chem. Soc.* **1972**, *94*, 6232 – 6233; b) N. Masciocchi, A. Sironi, D. D'Alfonso, *J. Am. Chem. Soc.* **1990**, *112*, 9395 – 9397.